Sustainable Food Technology

ROYAL SOCIETY OF CHEMISTRY

PAPER

View Article Online
View Journal

Cite this: DOI: 10.1039/d5fb00696a

Valorization of rice straw residue for canthaxanthin production *via* sustainable bioprocessing

Devendra Pratap Singh, Priyanka, Tania Raheja, Saumya Singh, Neera Agarwal and Meena Krishania *

Canthaxanthin is an orange-coloured carotenoid pigment produced by several microorganisms and is known for its anti-cancer, antioxidant, and anti-inflammatory properties. However, canthaxanthin production *via* chemical routes poses significant health and environmental concerns. In this study, a sustainable process was developed for canthaxanthin production using acid-treated rice straw (ATRS) residue as a substrate. Encapsulation was performed using different wall materials to enable controlled release of canthaxanthin. The highest canthaxanthin yield (135 mg L^{-1}) was achieved from *Dietzia kunjamensis* after optimization using response surface methodology. Furthermore, ultrasonication enhanced pigment extraction in ethanol by 16.67%, followed by purification using column chromatography. The purified canthaxanthin exhibited an antioxidant activity of 47% in the DPPH assay and showed stability at pH above 2. Among the encapsulating agents tested, polyvinylpyrrolidone showed the highest encapsulation efficiency (75%). Encapsulated canthaxanthin was characterized using FTIR, SEM, and XRD analyses. The Higuchi model provided the best fit for release kinetics from the cyclodextrin–pectin blend matrix (R^2 = 0.97). Flowability of the encapsulated powder was evaluated using Carr index, Hausner ratio, and bulk density measurements. Overall, the produced canthaxanthin demonstrates strong potential as a bioactive colorant for applications in the food and nutraceutical sectors.

Received 17th October 2025
Accepted 4th February 2026

DOI: 10.1039/d5fb00696a

rsc.li/susfoodtech

Sustainability spotlight

This study focused on addressing two issues at once: canthaxanthin production from the acid-treated rice straw residue while also mitigating waste and minimizing the health risk due to the consumption of synthetic dye. Canthaxanthin not only leads to colored food products but also enhances the antioxidant properties of food products. Encapsulation of canthaxanthin into different food wall materials improves its release kinetics, which makes it perfect for utilization in the food industry. This process is best fit in the circular bioeconomy, which utilizes agro-waste and produces commercially viable bioactive compounds that meet the criteria of SDGs.

1 Introduction

Canthaxanthin, also known as 4,4′-diketo-β-carotene, has a vibrant orange appearance. It is a member of the carotenoid xanthophyll family.[1] For centuries, color has been a part of our daily existence. The market for dyes and pigments is projected to be worth USD 33.20–49.10 billion by 2027.[2] However, the majority of coloring agents and dyes used today are produced chemically. However, submerged fermentation (SmF) can yield more stable microbial pigments while avoiding contamination and requiring less control than solid-state fermentation (SSF).[3] The food sector has made extensive use of this approach for the production of pigments by using glucose or rice flour as the primary carbon source.[4] To lower the pigment production cost and promote sustainable raw material utilization, several studies have used plentiful agricultural waste materials (lignocellulosic materials) like rice straw, jackfruit seeds, bagasse from sugarcane, and corn cobs.[3] Rice straw (RS) is one type of biomass.[5] India produces 126.60 million metric ton (MMT) of RS and 22.40 MMT of rice.[5] Historically, RS leftovers have either been burned or allowed to naturally decompose in the fields; both of these methods have serious negative effects on the environment and the economy.[6]

The most important sensory component in food selection is vision since it allows one to evaluate the quality of food before consuming it. The inherent color of a food acts as a visual signal, training the brain to quickly identify acceptable and secure food types.[7] Artificial coloring is widely used in the world food supply chain. However, according to *in vivo* research, they can result in adverse effects such as allergies, asthma, and tumor growth. These chemicals have been most closely linked to toxicological concerns to human health throughout the past century. Nevertheless, because they are more affordable, stable, and vibrant than natural ones, the food sector employs them.[7] A

National Agri-Food and Biomanufacturing Institute (BRIC-NABI), Formerly CIAB, Knowledge City, Mohali 140306, India. E-mail: meena@ciab.res.in

previous study has reported the production of monascus pigments from the hydrolysate of rice straw by submerged fermentation.[3] Several studies have reported canthaxanthin production by different species of *Dietzia* as mentioned in Table 2. *Dietzia natronolimnaea* HS-1 and *Dietzia maris* AURCCBT01 produce canthaxanthin respectively using glucose as a carbon source.[4,8] The use of waste whey and hydrolyzed molasses has also been reported for canthaxanthin production.[9,10] In biological systems, canthaxanthin is synthesized from β-carotene employing β-carotene ketolase enzyme with echinenone serving as an intermediary xanthophyll.[11] Canthaxanthin has a ketone functional group, which is responsible for several biological activities like anti-oxidant, anti-cancer, anti-inflammatory, and anti-aging properties.[1] Owing to these properties, it has attracted considerable market attention. A report showed that the pigment's market has grown from USD 135 million to USD 444 million with 2.6% CAGR from 2024 to 2032, and the Asia Pacific is a major player in the canthaxanthin market (GMI, 2025). Canthaxanthin is used in animal feed, food colourants, nutraceuticals, beverages, and cosmetics.[11] The WHO Expert Committee on Food Additives has recommended an ADI (Average Daily Intake) of canthaxanthin of 0.03 mg per kg BW. An expert committee of the European Food Safety Authority (EFSA) also agreed with this ADI.[12] Several companies like BASF (Germany), DSM (USA), Dynadis SARL (France), Novepha (China) and Taiyo Group (India) have commercial products around the world containing canthaxanthin.[11] This highlights the future potential and commercial viability of canthaxanthin.

Carotenoids are hydrophobic in nature, which makes it difficult for them to get solubilized in aqueous systems. Various approaches have been applied for the solubility enhancement of carotenoids, like encapsulation. Carotenoids like astaxanthin, canthaxanthin, β-carotene and many others act as guest molecules, while encapsulating agents like cyclodextrin (CD), maltodextrin (MD), pectin (PC) and protein hydrolysate act as host molecules. These host materials not only enhance the solubility of canthaxanthin, but also increase its shelf life, and preserve bio-activity and thermal and photo-degradation of carotenoids.[13] Various encapsulation techniques have been employed, including spray drying, freeze drying, emulsion-based methods, and electrospinning. Among these techniques, freeze drying is preferred over spray drying as it is more suitable for thermolabile products.[14]

Many studies have investigated canthaxanthin production in *Dietzia* strains; however, no study has been reported on canthaxanthin production by *Dietzia kunjamensis* using rice straw as a substrate. The aim of this study is sustainable production of canthaxanthin from the residual fraction of ATRS using *Dietzia kunjamensis*. Fermentations were systematically compared with acetate and citrate buffer-based media to determine the optimal buffer system for efficient saccharification and fermentation compatibility. To further enhance canthaxanthin production, the effects of different monovalent and divalent salts and nitrogen sources were evaluated during fermentation. In addition, the study investigated the antioxidant activity, pH stability, encapsulation efficiency, and release kinetics of purified canthaxanthin. To identify the best suitable encapsulating wall matrix for industrial applications, a comparative assessment of the Carr index (CI) and Hausner ratio (HR) was conducted for all encapsulating materials, with the aim of selecting a bioactive colorant for the food and nutraceutical sectors.

2 Materials and methods

2.1 Chemicals and reagents

All the solvents utilized in this study were of analytical grade and acquired from Sigma-Aldrich (USA). β-Glucanase (1 U mg^{-1}) from *Trichoderma longibrachiatum*, cellulase (0.8 U mg^{-1}) from *Aspergillus niger*, and HPLC grade canthaxanthin(>95% purity) were purchased from Sigma-Aldrich (USA). Sodium hydroxide (NaOH), MD,CD, sodium caseinate (SC), PC, polyvinylpyrrolidone (PVP), glucose and silica gel were purchased from CDH (New Delhi, India).Yeast extract (YE) was purchased from Hi-media (Maharashtra, India).

2.2 ATRS procurement and potential microbe isolation

ATRS was procured from the Food Engineering and Nutrition Lab, Center of Innovative and Applied Bioprocessing (CIAB), Mohali, Punjab, India. Soil was collected from CIAB (30.66836072641783, 76.72042073813246). To isolate pigment-producing microbes, stock solution of the soil sample was prepared by adding 1 g of soil in 100 ml water, and then serially diluting with nutrient agar media. Serially diluted samples were incubated for seven days at 32 °C (Memmert, Germany). After isolation of the desired pigment-producing strain, it was identified at Institute of Microbial Technology (IMTECH), Chandigarh, India.

2.3 Alkali treatment of ATRS and saccharification

Previously, ATRS generated after xylitol and prodigiosin production from hemicellulose content, by our research group,[15,16] was washed and dried in an oven (Memmert, Germany) at 45 °C for 7 h. A modified,[17] technique was used to treat 5% (w/v) dried ATRS with four different concentrations of NaOH (w/v), namely 1%, 2%, 3%, and 4%, at 121 °C for 15 min. Alkali treated ATRS was washed and dried. 3% (w/v) of alkali treated residue was saccharified with 0.5 mM acetate and 0.5 mM citrate buffer[18,19] with three different combinations of β-glucanase and cellulase enzymes at 52 °C for 72 h at 150 rpm in a shaker with 0.2% (w/w) enzyme loading (Innova 42, New Brunswick, USA). In the first combination β-glucanase and cellulase were taken in a 65 : 35 ratio, in the second combination an equal ratio of both enzymes was used, and in the third combination a 35 : 65 ratio was used. Glucose concentration was determined by HPLC (Agilent Infinity 1290, California, USA) in a HiPlexH column (Agilent, California, USA) using a 5 mM H_2SO_4 mobile phase with a 0.6 ml min^{-1} flow rate, and column temperature was maintained at 65 °C.

2.4 Canthaxanthin production by SmF

Canthaxanthin was produced by using saccharified glucose from ARTS as a carbon source with acetate and citrate buffer at

neutral pH.[4] Prepare 30 ml seed culture in nutrient broth with 10 g per l commercial glucose at 150 rpm and 32 °C in a 100 ml flask. After 96 h, seed culture was used as the inoculum for canthaxanthin production. Furthermore, the standard curve was plotted with lyophilized dry cell biomass against O.D, for the determination of cell biomass concentration in a fermented broth at 600 nm by UV-vis spectroscopy. Colour difference due to acetate and citrate buffer was measured by using a handheld spectrophotometer (RM200, Lovibond, China). Colour parameters L^*, a^*, b^*, and C^* were selected from Commission Internationale de l'Eclairage (CIE). L^* represents lightness and darkness of the sample; if the a^* value is positive it showed redness while negative a^* represents greenness, positive b^* represents yellowness while negative represent blueness of the sample and C^* represents chroma of the sample. The effect of the nitrogen source and salt concentration on the biomass production was also determined.

2.5 Optimization of pigment production

Optimization of canthaxanthin production was done by the Design Expert software (version 12.0.11.0, Stat-Ease, Inc., Minneapolis, USA). In the present study, the experiments were performed in 100 ml conical flasks with 30 ml media under conditions of RPM: 150 rpm, time: 120 h and temperature: 32 °C. For detailed optimization, five independent parameters were selected for optimization within a certain range: glucose concentration (1–2.5%, w/v), YE (0.5–2% w/v), NaCl (0.5–1.5%, w/v), pH (6–8), inoculum concentration (0.5–2.5%, v/v). These parameters were coded as *A*, *B*, *C*, *D* and *E*, respectively. Statistical analysis was performed using an ANOVA table generated by Design Expert software.[4,16]

2.6 Extraction and purification of the intracellular pigment

Microbial cell biomass was concentrated using a centrifuge (Sorvall ST8R, Thermo scientific, USA) from fermented broth and the intracellular pigment was extracted in 100% ethanol with and without bath ultrasonication (Sonica Ultrasonic Cleaners, Soltec, Italy) at 40 °C for 45 min.[20] Silica gel column chromatography was used to purify the raw pigment. Different pigment fractions were separated using silica with pore sizes of 60 Å and mesh sizes of 200–400. For elution, 4–40% (v/v) ethyl acetate in hexane was used to obtain the pure form of the pigment canthaxanthin.

2.7 Characterization of the pigment

2.7.1 UV-vis spectrophotometer. The purified pigment was dissolved in ethanol and characterized by using a UV-vis Spectrophotometer (UV-1900i SHIMADJU, Japan) with standard canthaxanthin in the spectrum range of 350 nm to 600 nm.

2.7.2 TLC (thin layer chromatography). For the TLC analysis, the sample and standard were spotted on a pre coated silica gel plate (Merck, USA). Hexane and ethyl acetate were used as the mobile phase in a 6 : 4 ratio. The R_f value was calculated by using the formula described by Miglani *et al.* (2023).[16]

$$R_f = \frac{\text{disance travel by solute}}{\text{distance travel by solvent}} \quad (1)$$

2.7.3 UPLC (ultra performance liquid chromatography). The purified pigment was further validated by UPLC (Waters, Milford, MA, USA) with standard canthaxanthin; the ratio of acetonitrile and methanol in a 7 : 3 ratio was used as the mobile phase in a C18 reverse phase column (Agilent Zorbax eclipse plus C18, USA).10 µl sample was injected with a flow rate of 0.8 ml min^{-1} at 30 °C.[21]

2.7.4 MS (mass spectrometer). The purified pigment fraction and standard canthaxanthin were dissolved in ethanol. The mass (m/z) range selected from 450–650 m/z ratio in MS (6120, Agilent, USA). Electron spray ionization (ESI) and a quadrupole mass analyzer detector were operated in scan mode for the detection of the m/z ratio of the purified pigment and standard.[22]

2.8 Encapsulation of canthaxanthin in different wall materials

Various encapsulating wall materials were used to encapsulate purified canthaxanthin for use in food applications. The modified[16] method was used for the encapsulation; various wall materials, including MD, CD, SC, PC, and PVP, were employed. Each of these wall materials can be used separately and in combination with PC to create a higher-quality encapsulated product. After dissolving 300 mg of wall material each in 20 ml of 70% (v/v) ethanol with 1 mg of core material, the mixture was agitated at 400 rpm for five hours at 50 °C. The same conditions were used when 50 mg more of PC was added to each wall material. After stirring, the solution was sonicated for 2 min, and solvent was evaporated and freeze-dried to obtain the encapsulated final product. Encapsulation efficiency was calculated by using formula (2).[23]

$$\text{Encapsulation efficiency}(\%) = \frac{\text{total canthaxanthin} - \text{surface canthaxanthin}}{\text{Theoretical canthaxanthin}} \times 100 \quad (2)$$

For total canthaxanthin content determination, 2 mg of the encapsulated product was dissolved in 100% ethanol, and vortexed for 10 min followed by centrifugation at 7500 rpm for 10 min. The supernatant was filtered by using a 0.45 µm filter and absorbance was calculated at 475 nm for the canthaxanthin determination. For determination of surface canthaxanthin content, 2 mg encapsulated material was dissolved in 1 ml of hexane and vortexed for 5 s and filtered. Absorbance was measured at 475 nm and concentration was determined.

2.9 Characterization of the encapsulated material

2.9.1 FTIR (Fourier transform infrared) spectroscopy. The interaction study between the pigment and wall materials was done by FTIR (IRSpirit-X, Shimadzu, Kyoto, Japan). The scan range was set between 500 nm and 4000 nm with 32 scans per sample.

2.9.2 XRD analysis. The crystalline structure of wall materials and the encapsulated core material was determined (Smartlab SE, Rigaku, Japan) by XRD and the scatter (2θ) range was from 5° to 50° with a scanning speed of 15° min^{-1}.[24] The standard wall materials and encapsulated materials were placed on a quartz plate for XRD analysis.

2.9.3 SEM analysis. For the morphological analysis of each of the encapsulated products and standards, 1 mg of each sample was placed on carbon tape for gold sputtering. After sputtering, the samples were analyzed by using a SEM microscope (JEOL6000 Benchtop, Japan).[25]

2.10 Release kinetics of encapsulated canthaxanthin

For the release of canthaxanthin from the encapsulated matrix, different kinetic models were evaluated. For the release of canthaxanthin, a modified method by Mahalakshmi *et al.* (2020) was used;[23] briefly, 50 mg of encapsulated powder was dissolved in phosphate buffer with 1% (v/v) tween 80 at pH 7.2. The solution was placed on a magnetic stirrer at 300 rpm for 2 h and at room temperature. 1 ml sample was taken at intervals of 30 min to maintain the total volume. 1 ml fresh solution was added at every interval and canthaxanthin content was determined based on UV absorbance. The release kinetics of canthaxanthin were evaluated using zero-order (eqn (3)), first-order (eqn (4)), second-order (eqn (5)), and Higuchi models (eqn (6)), as described by Li *et al.* (2024).[26]

$$A = -k_t + A_0 \tag{3}$$

$$\ln(A) = -k_t + \ln(A_0) \tag{4}$$

$$\frac{1}{[A]_t} = k_t + \frac{1}{[A]_0} \tag{5}$$

$$Q = k_H\sqrt{t} \tag{6}$$

where A was the released canthaxanthin after time t, A_0 was the initial encapsulated canthaxanthin, k was the rate constant, Q was the cumulative release canthaxanthin and k_H was the Higuchi dissolution constant.

2.11 pH stability

pH stability of the pigment was determined in the pH range of 2–12. Purified canthaxanthin was dissolved in ethanol and pH was adjusted by using 1 M HCl and 1 M NaOH.[27]

2.12 Antioxidant activity determination

Antioxidant activity of the purified pigment was determined by a modified method of Castangia *et al.* (2022);[1] 0.5 mM solution of DPPH was prepared. The 200–800 μg ml^{-1} range of purified canthaxanthin was also prepared. An equal amount of DPPH and pigment was dissolved and incubated for 30 min in the dark; and absorbance was obtained at 517 nm. DPPH activity was determined by using the formula:

$$\%\ \text{DPPH activity} = \left(\frac{(A_c - A_s)}{A_c} \times 100\right) \tag{7}$$

A_c-absorbance of control (DPPH dissolved in methanol); A_s-absorbance of the sample.

2.13 Water activity (a_w), Carr index (CI) and Hausner ratio (HR)

Flowability and compressibility of the encapsulated pigment in different food matrices were calculated by using the HR and CI value modified formula.[28] For the estimation of the HR, bulk and tapped volume were calculated by using a tapped density meter (Tap Density Tester, QS-2010, Mumbai, India). The instrument's measuring cylinder was filled with 2 g of each sample, and tap was set at 250 tap per min under rotating conditions for one minute with 3 mm stroke length. Bulk and tapped volume of the powder were noted. A CI of less than 15% is considered as very good, 15–20% is good, 20–35% is fair, 35–45% is bad and more than 45% is considered as very poor flowability.[29]

$$\text{HR} = (V_{bulk}/V_{tapped}) \tag{8}$$

$$\text{CI} = ((V_{bulk} - V_{tapped})/V_{tapped}) \times 100 \tag{9}$$

V_{bulk} was the bulk volume and V_{tapped} was the tapped volume of the sample.

Water activity of the encapsulated pigment was determined by using a water activity meter (Lab Swift, Novasina, Switzerland) at room temperature. Two-thirds of the sample tray was filled with the sample.

3 Results and discussion

3.1 Isolation and phylogenetic analysis of the pigment-producing strain

A variety of colored colonies were obtained by plating a serially diluted sample of soil on a nutrient agar plate. One orangish red coloured colony was selected, because it provides the visual hint of canthaxanthin presence in microbial species.[30] Combining morphological traits, biochemical testing and 16S rRNA gene sequence analysis, the pigment-producing strain was determined to be *Dietzia kunjamensis*. A phylogenetic tree was constructed by the by neighbor-joining method and evolutionary distance was calculated by the maximum composite likelihood method in MEGA X. The phylogenetic tree and microscope image of *Dietzia kunjamensis* is shown in SI Fig. 1.

3.2 Alkali treatment and saccharification of ATRS

Maximum glucose concentration was obtained in the sample treated with 4% (w/v) alkali *i.e.* 58% (w/v) in 72 h. 77.75% (w/v) xylose recovery was noticed in liquid hydrolysate from hemicellulose of RS, following dilute acid pretreatment, as reported in a previous study by our research group,[15] while keeping lignin and cellulose contents intact. A previous study showed the synergetic effect of 0.5% (v/v) H_2SO_4 and 1.5% (w/v) NaOH and recovered 30.3% (w/v) of glucose on saccharification of RS. During autoclaving, H_2SO_4 created hydronium ions that broke down hemicellulose and left behind xylan and broken fibers of

RS.[16] Alkali treatment released the lignin and loosened cellulose by solvation and saponification of RS, thus easing the accessibility of cellulase and β-glucanase enzymes for saccharification. Increasing the amount of NaOH improved glucose recovery up to a certain point, as shown in SI Fig. 2. A previous study showed that a combination of acid and alkali treatment yielded 353.1 mg per g glucose from RS derived cellulose, which is less than that in our study.[31] An enzyme ratio of cellulase and β-glucanase of 65 : 35 showed better glucose recovery as compared to the other two combinations. β-Glucanase helps to cleave the internal bond, which generates reducing and non-reducing ends, while cellulase helps to cleave at the terminal of cellulose fibers.[32] Substrate loading for saccharification was kept at 3% (w/v) because a previous study showed that high substrate loading decreases the glucose yield due to the increase in viscosity of the slurry, and limitations in mass transfer and product inhibition.[32]

3.3 SmF for canthaxanthin production

Cell growth in the seed culture reached 6.72 mg ml^{-1} after 96 h, and this culture was subsequently used as the inoculum for the next set of experiments. Initially fermentation was done in media comprising 15 g per l glucose, 10 g per l YE and 5 g per l NaCl at 32 °C under 150 rpm shaking conditions at pH 7. Glucose was completely consumed at 144 h, and maximum biomass was obtained at 120 h as shown in Fig. 1. The culture medium was further supplemented with 10 g per l peptone as an additional nitrogen source to enhance the production of canthaxanthin. Peptone supplement was unable to enhance the canthaxanthin production, as previously reported.[33] However, excess nitrogen source enhanced the protein synthesis while nitrogen deficient conditions increase the synthesis of energy rich molecules like lipids. Lipid molecules capture the apolar carotenoids and flux out from the metabolic pathway thus minimizing product inhibition.[33] Monovalent salts showed more biomass yield as compared to divalent salts as shown in SI Fig. 3. In the presence of monovalent salt, NaCl showed

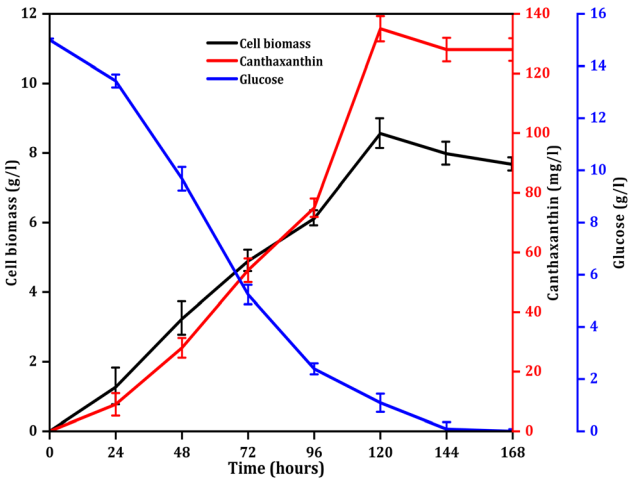

Fig. 1 Glucose consumption, cell biomass growth profile and canthaxanthin production.

Table 1 Colour value of fermented broth in different buffer systems and the control

Sr. no.	Colour parameter	Acetate buffer	Citrate buffer	Control
1	L^* (lightness)	29.60 ± 0.5	20.70 ± 0.4	41.60 ± 0.07
2	a^* (redness)	14.72 ± 0.7	18.27 ± 0.9	25.30 ± 0.08
3	b^* (yellowness)	24.76 ± 0.4	18.60 ± 0.1	46.00 ± 0.05
4	C^* (chroma)	28.81 ± 0.3	26.18 ± 0.8	51.30 ± 0.10

enhancement in biomass yield as compared to KCl. This is because NaCl has a strong effect on the membrane, which helps in more substrate uptake.[34]

For the canthaxanthin production from ATRS-derived glucose, after saccharification, glucose was filtered by vacuum filtration, and the pH was adjusted with 1 M NaOH. However, when the glucose concentration was made equal for both acetate and citrate buffer, the subsequent canthaxanthin production was nearly the same in both buffer systems. This yield was about 20% lower than the yield achieved when using commercial glucose as a control, which was further confirmed by the increased colour values in the control. But colour values of acetate buffer and citrate buffer were different; citrate buffer had a dull appearance as compared to acetate buffer and this was further confirmed by the L^* values of citrate and acetate buffer of 20.70 and 29.70 respectively. Lower L^* and C^* values in citrate buffer were observed because citric acid is stronger than acetic acid and can chelate with the trace metal elements present in YE, resulting in browning of the media, which appeared darker and redder than acetate buffer.[35] Chroma is related the colour saturation, which is high in the control sample, while acetate chroma is better than that of citrate, which signifies that acetate buffer is better than citrate buffer for canthaxanthin production. Redness in acetate buffer decreased, but yellowness and chroma increased as compared to those of the citrate buffer; both buffer systems were compared with commercial glucose used for fermentation as a control. Colour values of buffer and synthetic media are given in Table 1. Citric acid and acetic acid are both weak acids, and their undissociated forms can easily pass through the plasma membrane and dissociate in the cytosol lowering the intracellular pH of cells, which is limiting the growth of cells.[36] Thus, this results in a decrease in canthaxanthin production in acetate and citrate buffer-derived glucose fermentation as compared to commercial glucose fermentation, which was further supported by a decrease in L^*, a^*, b^* and C^* colour values in both acetate and citrate buffer fermentation.

3.4 Optimization of canthaxanthin production

The determination and statistical optimization of the significant variables influencing canthaxanthin production was conducted using the central composite design (CCD) model of RSM. RSM was used to evaluate the impact of the input conditions and their interactions on the output (canthaxanthin concentration) (Fig. 2). Under optimized conditions, 8.54 g per l biomass was obtained which is the highest for this strain;

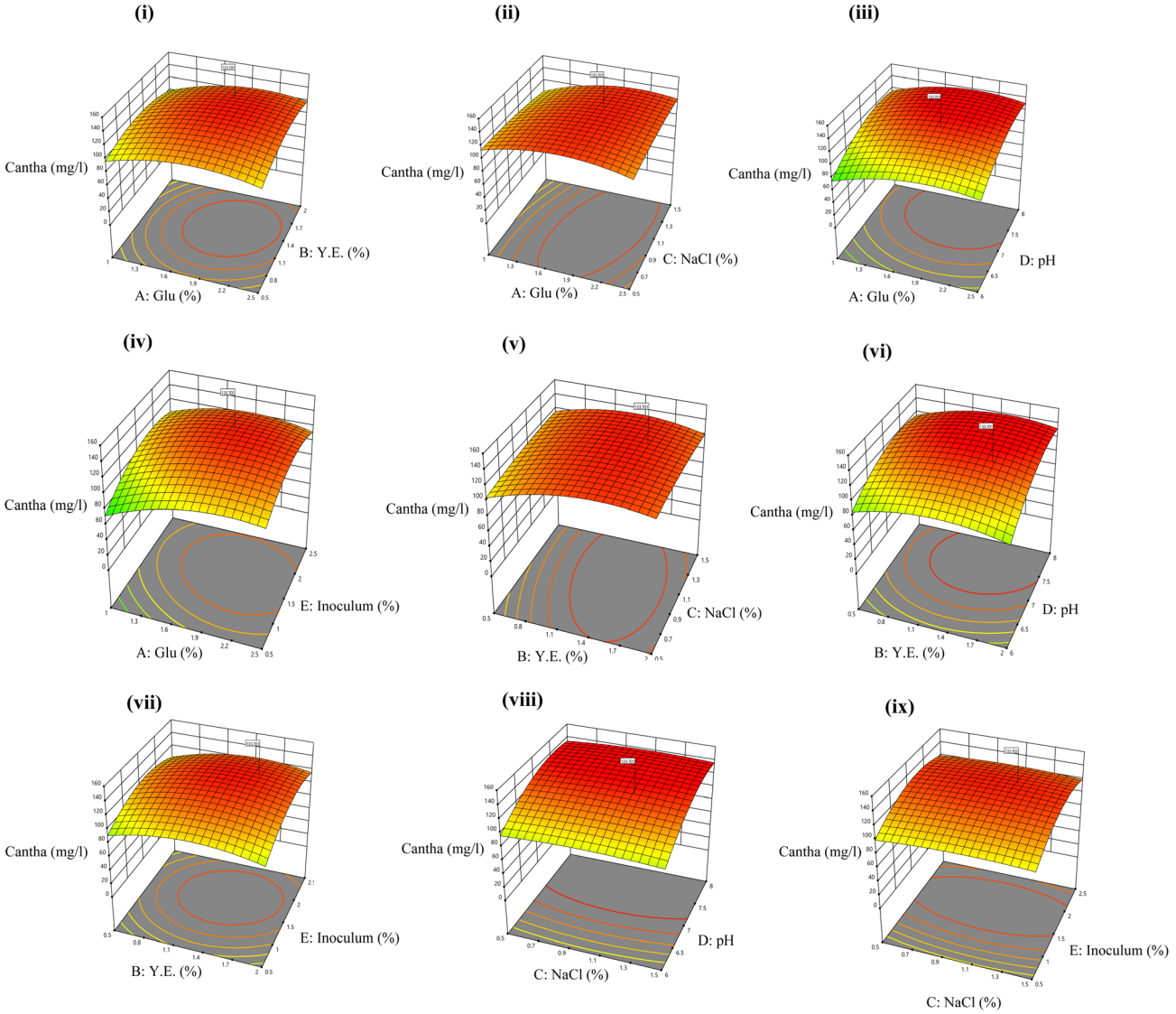

Fig. 2 3D RSM plots showing the impact of interaction of input parameters on canthaxanthin production namely (i) AB, (ii) AC, (iii)AD, (iv) AE, (v) BC, (vi) BD, (vii) BE, (viii) CD, and (ix) CE.

previously reported canthaxanthin production by different strains is shown in Table 2. The best optimized set of conditions out of 50 runs was 1.75% (w/v) glucose, 1.25% (w/v) YE, 1% (w/v) NaCl, pH 7 and 1.5% (v/v) inoculum size, which led to 135 mg l^{-1} yield of canthaxanthin. A pigment to biomass yield of 0.015 $g_{pigment}$ $g_{DCW}{}^{-1}$ was observed. A previous study reported the highest canthaxanthin production from *Dietzia maris* NIT-D which showed 7.39 g l^{-1} of biomass and 122 mg l^{-1} of canthaxanthin.[37] The following equation established the relationship between canthaxanthin yield and variables of the model:

$$Y = -955.43 + 95.07A + 32.89B + 11.34C + 241.04D + 74.10E + 5.61AB + 14.75AC - 0.79AD - 7.92AE - 9.75BC + 4.45BD$$

Table 2 Comparative study of canthaxanthin production

Sr. no.	Name of the organism	Substrate	Yield (mg l^{-1})	References
1	*Dietziakunjamesis*	Glucose	135	Present study
2	*Dietzia maris* NIT-D	Glucose	122	37
3	*Dietzia natronolimnaea* HS-1	Enzymatic hydrolysed molasses	14.63	10
4	*Dietzia natronolimnaea* HS-1	Whey lactose	2.9	9
5	*Dietzia maris* AURCCBT01	Glucose	3.1	4
6	*Dietzia natronolimnaea* HS-1	Glucose	4.99	38

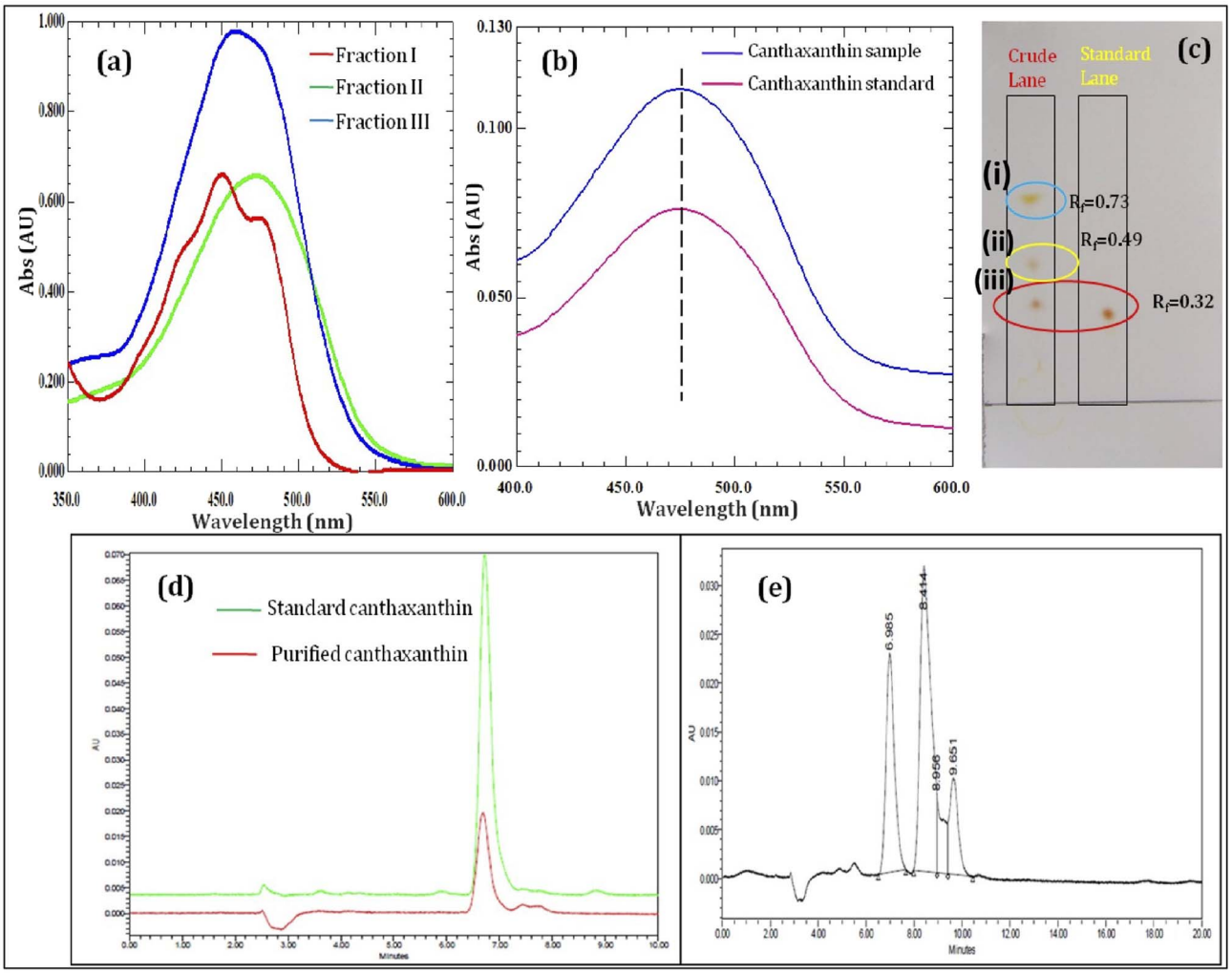

Fig. 3 (a) Different fractions of the pigment, (b) UV-vis spectrum of standard and sample canthaxanthin, (c) TLC of the crude extracted pigment and standard canthaxanthin, (d) UPLC chromatogram showing overlapped peaks of standard and sample canthaxanthin, and (e) crude pigment peaks in UPLC.

$$+ 3.12BE + 1.43CD - 1.06CE + 0.09DE - 26.11A^2 - 24.85B^2 - 15.25C^2 - 16.36D^2 - 18.66 \times 10^2 \quad (10)$$

where Y is the canthaxanthin yield (mg l^{-1}) and A, B, C, D, and E are independent input variables of the model; the R^2 value of the model appeared to be 0.99 whereas predicted and adjusted R^2 values were 0.97 and 0.98 respectively in the suggested quadratic model. The p-value of the model was less than 0.0001, which showed the significance of the model at the 95% confidence level. The p-value of pair interactions of AB, AC, AE, BC and BD was significant for this model while that of AD, BE, CD, CE and DE was insignificant (SI Table 1). The F-value of the model was 240.67, which indicates that the model is significant and there is only 0.01% chance of error due to noise.

3.5 Extraction and purification of the pigment

Canthaxanthin was extracted in ethanol with ultrasonication at 40 °C for 45 min, and absorbance was analyzed at 475 nm every 15 min. The non-sonicated sample treated under similar conditions was considered as the control. The ultrasonicated sample showed higher absorbance as compared to the non-sonicated sample. However, in both the samples, absorbance did not increase after 45 min. The ultrasonicated method showed 16.67% more pigment extraction as compared to the control. Ultrasonic waves work on acoustic cavitation; when ultrasound waves pass through a liquid medium, it generates alternating low and high pressure cycles, which form microscopic bubbles. When these microscopic bubbles collapse, they disrupt the cell wall, leading to the release of intracellular canthaxanthin in ethanol.[39] The extracted pigment was further purified with silica gel column chromatography using hexane and ethyl acetate as the mobile phase. Ethyl acetate concentration from 4% (v/v) to 40% (v/v) was used with hexane to get the different pigment fractions as shown in Fig. 3(a). The first fraction is possibly β-carotene which is an intermediate product in canthaxanthin biosynthesis.[40]

3.6 Characterization of the pigment

3.6.1 UV-vis spectrophotometer. The purified pigment fraction and standard canthaxanthin showed maximum UV-vis

absorbance at 474 nm as shown in Fig. 3(b). A previous study showed that canthaxanthin UV absorbance ranges from 468 nm to 475 nm in cyclohexane.[41]

3.6.2 TLC. Three different bands were observed on a TLC plate. These bands showed R_f values of 0.32, 0.49 and 0.79. The standard canthaxanthin showed a similar R_f value *i.e.* 0.32 to sample canthaxanthin as shown in Fig. 3(c) spot (iii). Canthaxanthin co-produce along with β-carotene in the *Dietzia natronolimnaea* HS-1 (ref. 40) spot (i) was β-carotene with R_f value 0.73, and also detected in MS, while spot (ii) unknown pigment.

3.6.3 UPLC analysis. The crude extracted pigment showed three different peaks as shown in Fig. 3(e), while purified canthaxanthin exactly overlapped with the standard canthaxanthin as shown in Fig. 3(d), confirming it to be canthaxanthin. In the extract the canthaxanthin has 69% area with 8.25 retention time and β-carotene with 19% area eluted at 6.96 min, while the remaining area corresponds to an unknown pigment in the ethanolic extract.

3.6.4 MS analysis. The ESI method was used to protonate the purified sample and standard canthaxanthin. The molecular weight of canthaxanthin is 564.8, that of the protonated $[M + H]^+$ form of purified canthaxanthin was 565.2, and that of the standard canthaxanthin was 565.8. Canthaxanthin has a keto functional group, which helps to obtain the protonated form. This result aligns with the previous reports.[22,42] Toluene (M_W: 92 amu), xylene (M_W: 106), water (M_W: 18) and acetic acid (M_W: 60) are the products which are eliminated during the fragmentation process of xanthophylls.[43] Purified pigment mass (m/z) at 459.2 $[(M + H)^+ - 106]$ showed xylene elimination from purified canthaxanthin, while standard canthaxanthin showed elimination of acetic acid $[(M + H)^+ - 60]$, as revealed by the peak at 505.8 as shown in SI Fig. 4(a and b). Other than canthaxanthin, the column purified first fraction showed an m/z value of 537.6, which corresponds to the presence of β-carotene in the extracted pigment, as shown in SI Fig. 4(c).

3.7 Encapsulation efficiency (EE)

The highest EE was observed in 75% PVP whereas the lowest was observed 3% in SC incorporated with PC. MD (62%), SC (46%) and PVP showed improved EE when canthaxanthin was encapsulated individually but EE decreased when incorporated with PC as shown in SI Table 2. PC has an adhesive nature, which could result in a decrease in EE.[44] In the CD treated sample, the EE was greatly improved by adding PC from 24% to 54%. CD has a cage like structure with a hydrophobic core, which facilitates the interaction of hydrophobic canthaxanthin, and PC addition improved the EE. PC individually showed 35% EE of canthaxanthin. A previous study showed 73% canthaxanthin encapsulation in MD by the spray drying method.[40] Hydrolysate of soy protein showed 77.46% EE,[45] while another study showed 70.60% EE in an alginate – high methoxy pectin emulsion.[46]

3.8 Characterization of encapsulates

3.8.1 FTIR analysis. FTIR analysis was used to determine how the wall and core materials interacted. All the standard and wall materials showed a stretch in the common spectrum range of 3200–3600 cm^{-1} which mainly showed O–H vibrational stretching.[47,48] As per the previous studies, CH_2 vibration stretching has been observed between 2910 and 2945 cm^{-1} for all standards (PC 2939 cm^{-1}, CD 2925 cm^{-1}, MD 2913 cm^{-1}, SC 2916 cm^{-1} and PVP 2917 cm^{-1}).[43,48–50] Purified canthaxanthin showed symmetrical and asymmetrical vibrations at 2849 cm^{-1} and 2917 cm^{-1} respectively as shown in Fig. 4(a). Asymmetrical vibration of the C=O group was observed at 1731 cm^{-1} while CH_2 scissoring was observed at 1471 cm^{-1}. In encapsulated CD with canthaxanthin, the intensity of the characteristic peaks of carbohydrate at 1018 cm^{-1}, 1077 cm^{-1}, and 1155 cm^{-1} did not change much, but adding PC enhanced the intensity of these peaks as shown in Fig. 4(b). On adding PC, the 1155 cm^{-1} wavenumber changed to 1149 cm^{-1} which showed interaction.[44] In the case of MD, the characteristic peaks of the standard at 924 cm^{-1}, 1077 cm^{-1} and 1147 cm^{-1} were observed. The encapsulating core material enhanced the intensity but no significant shift in peaks was seen even after adding PC as shown Fig. 4(c). A similar interaction was also previously reported.[51] The characteristic peak of canthaxanthin at 1731 cm^{-1} disappeared in MD which showed the formation of hydrogen bonding with MD. The standard SC showed characteristic peaks at 1600 cm^{-1} to 1200 cm^{-1}, C=O and N=H vibration was observed at 1582 cm^{-1} and 1500 cm^{-1} respectively.[52] When canthaxanthin was encapsulated in SC, characteristic peaks of SC disappeared; in contrast, addition of PC with SC, resulted in the reappearance of the peak as shown in Fig. 4(d). It might be pectin which was stabilizing the deformation of SC during the encapsulation process. In the case of standard PVP, the peaks were observed at 1656 cm^{-1}, 1420 cm^{-1}, and 1275 cm^{-1}. The peaks at 1656 cm^{-1} and 1275 cm^{-1} are attributed to vibration stretch of C=O and C=N or CH_2 twisting respectively. On binding with canthaxanthin, the 1656 cm^{-1}, peak shifted to 1652 cm^{-1} as shown in Fig. 4(e) which validated binding of canthaxanthin with PVP.[53] Canthaxanthin encapsulation in PC led to peak shifting from 1050 cm^{-1} to 1016 cm^{-1} which showed encapsulation of canthaxanthin in PC. The characteristic peak at 1731 cm^{-1} disappeared as shown in Fig. 4(a).

3.8.2 XRD characterization. Encapsulation of the pigment in the wall material changes the crystalline structure of wall materials. The standard CD structure showed peaks at 6.3, 9, 10.7, 12.5, 17.8, 22.8, and 27.2° showing the crystalline nature of CD. The intense peak at a lower 2θ value and a lower peak at a higher 2θ value validate the cage like structure of CD which was previously reported.[24] On encapsulation of canthaxanthin in CD, the crystalline peak of standard CD changed, which is due to hydrogen bonding between the polar group of canthaxanthin and CD.[54] In the mixture of PC and CD, more peak broadening and a decrease in the intensity of peak were observed, which revealed the amorphous structure of encapsulated powder as shown in Fig. 5(a). A broader peak was observed in the MD which corresponds to the amorphous structure.[55] Encapsulating the core material in MD alone and in a mixture of PC and MD did not change the amorphous nature of encapsulated MD which is shown in Fig. 5(b). MD has a disordered structure, which resulted in peak broadening,

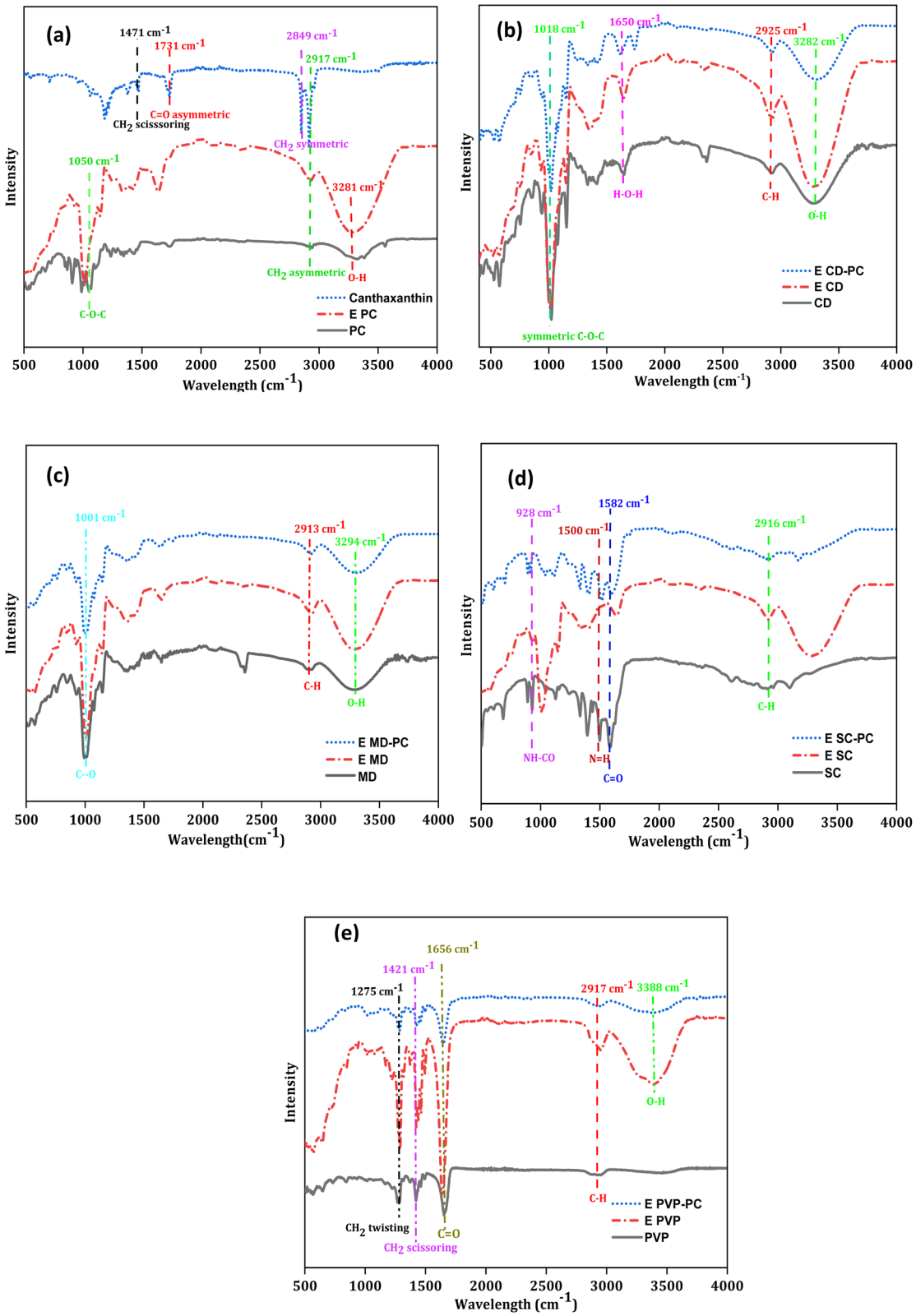

Fig. 4 FTIR analysis of encapsulated canthaxanthin in (a) PC and canthaxanthin, (b) CD, (c) MD, (d) SC, and (e) PVP.

which is a characteristic of an amorphous material.[56] In the case of standard SC, the 2θ values were observed at 21.6 and 25.1° and some broadened peaks were observed beyond 25°, which showed the crystalline nature of this wall material. These peaks get diminished when encapsulated with canthaxanthin which indicate hydrogen bonding of canthaxanthin with SC.[57]

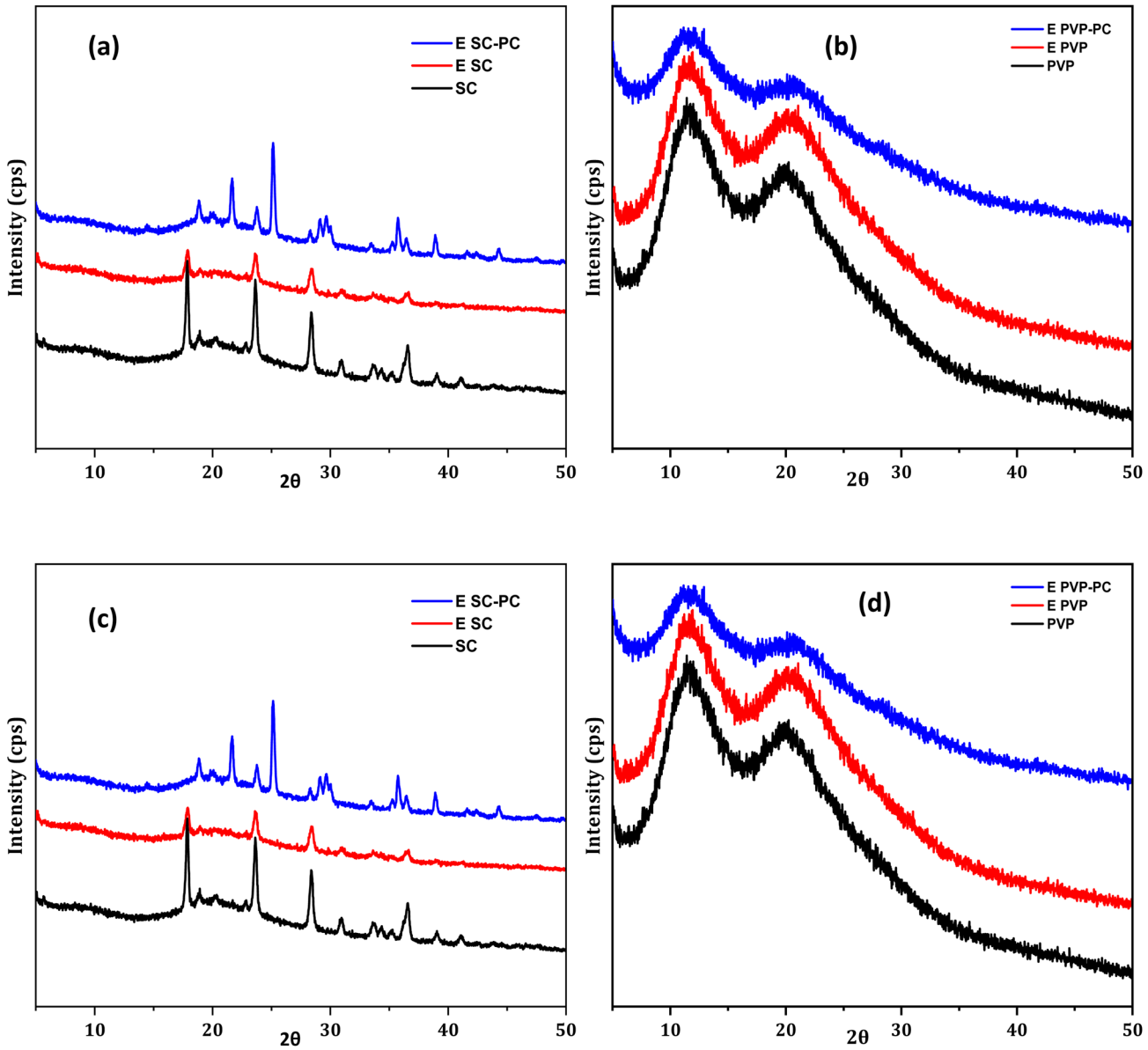

Fig. 5 XRD analysis of canthaxanthin encapsulated in (a) CD, (b) MD, (c) SC and (d) PVP.

Crystallinity of SC with canthaxanthin increased when it was incorporated with PC, which has a semi-crystalline structure.[58] The major peak intensities were observed at 17.8, 23.6 and 28.4° which showed improved crystallinity of encapsulated SC when added with PC. Broad peaks in standard PVP were observed at 11.2 and 20.2° which showed the amorphous nature of PVP.[59] On encapsulating canthaxanthin in PVP no change was observed in the peak but intensity decreased. Pectin incorporation in PVP also did not change the peak value but enhanced the intensity of peaks at 11.2 and 20.2° which was an amorphous characteristic of an encapsulated material as shown in Fig. 5d.

3.8.3 SEM analysis. SEM analysis of encapsulated powder showed structural changes in each wall material. In the case of CD, hydrogen bonding of canthaxanthin with the core of CD formed a flocculant structure while adding PC with CD improved the surface as shown in Fig. 6a(iii). Standard MD showed a structured arrangement, while on freeze drying, stress developed due to sublimation of water, resulting in its wrinkle sheet like surface as shown in Fig. 6b(iii).[60] Standard PVP showed round irregular surface morphology, while on encapsulation, canthaxanthin thin sheets were observed in PVP and PVP with PC (Fig. 6c(iii)). When canthaxanthin was encapsulated in SC, the morphology of SC changed from a sponge like structure to agglomerates, while adding PC made a protective layer on it, making a clump like structure, hence reducing the encapsulation of canthaxanthin[61] as shown in Fig. 6d(iii).

3.9 Release kinetics of canthaxanthin

The release kinetics of canthaxanthin varied in different matrices. The fastest release was observed in SC, while MD showed the slowest canthaxanthin release. After 30 min of stirring, almost

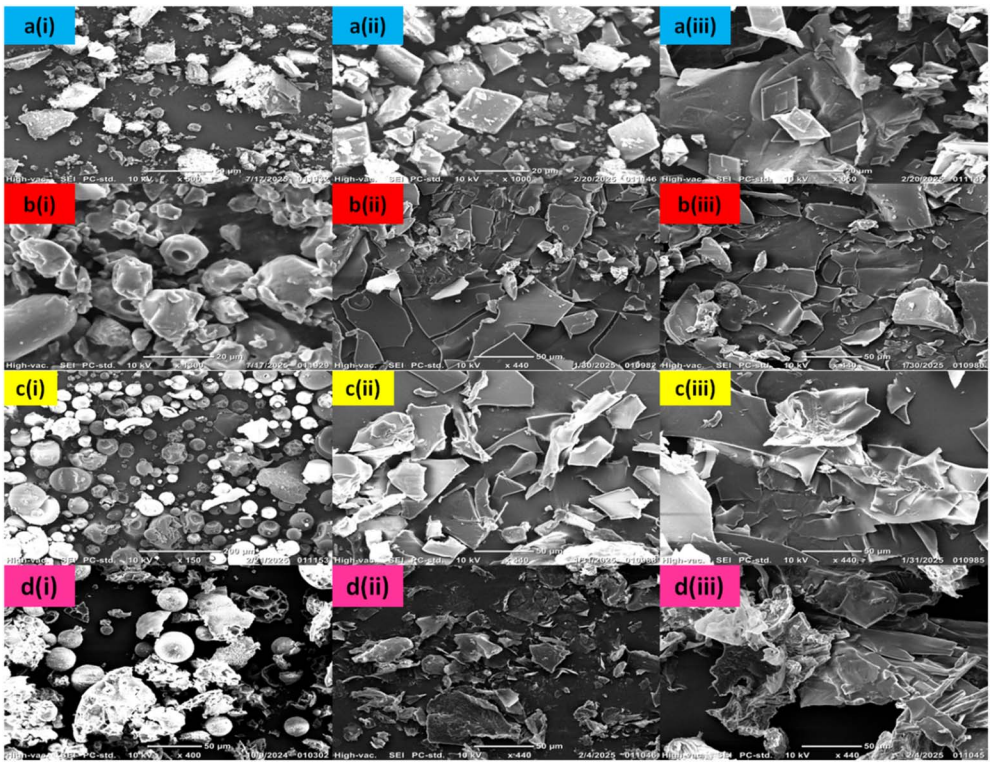

Fig. 6 SEM micrographs of (a(i)) standard CD, (a(ii)) canthaxanthin encapsulated in CD, (a(iii)) canthaxanthin encapsulated in CD–PC, (b(i)) standard MD, (b(ii)) canthaxanthin encapsulated in MD, (b(iii)) canthaxanthin encapsulated in MD–PC, (c(i)) standard PVP, (c(ii)) canthaxanthin encapsulated in PVP, (c(iii)) canthaxanthin encapsulated in PVP–PC, (d(i)) standard SC, (d(ii)) canthaxanthin encapsulated in SC, and (d(iii)) canthaxanthin encapsulated in SC–PC.

more than 95% of the canthaxanthin was released in both cases (individual SC and SC incorporated PC). The R^2 value of experimental fitted data in shown in Table 3; in different models, the highest R^2 value was 0.97 obtained for the MD in the Higuchi model and for PVP R^2 was found to be 0.95 in the same model. The least fit R^2 value was found for the SC in all the models.

3.10 pH stability

For the food application, a compound must be stable in a wide pH range. The purified pigment was tested in the pH range of 2 to 12. Under acidic conditions, the pigment colour changed significantly, but under basic conditions, no colour change was observed. At pH 2, the pigment degraded and turned colourless after 15 h, which was further confirmed by the UV-vis spectrophotometer spectrum as shown in Fig. 7(b–f). A previous study reported that canthaxanthin degraded at high concentrations of trifluroacetic acid (>0.1 M); acidic conditions help in protonation of carotenoids which results in colour loss and peak broadening of carotenoids.[62]

3.11 Antioxidant activity

Carotenoids show antioxidant activity due to the presence of a functional group and long polyene chain. In the case of canthaxanthin, it has a C=O functional group and 13 double

Table 3 R^2 value of release kinetics of canthaxanthin in different matrices

		R^2			
S. no.	Encapsulating matrix	Zero order	First order	Second order	Higuchi model
1	CD	0.81	0.77	0.76	0.88
2	MD	0.96	0.91	0.83	0.97
3	SC	0.61	0.61	0.61	0.70
4	PVP	0.92	0.90	0.87	0.95
5	PC	0.91	0.91	0.91	0.88
6	CD–PC	0.89	0.89	0.90	0.88
7	MD–PC	0.87	0.73	0.69	0.86
8	PVP–PC	0.86	0.84	0.82	0.92
9	SC–PC	0.89	0.89	0.89	0.91

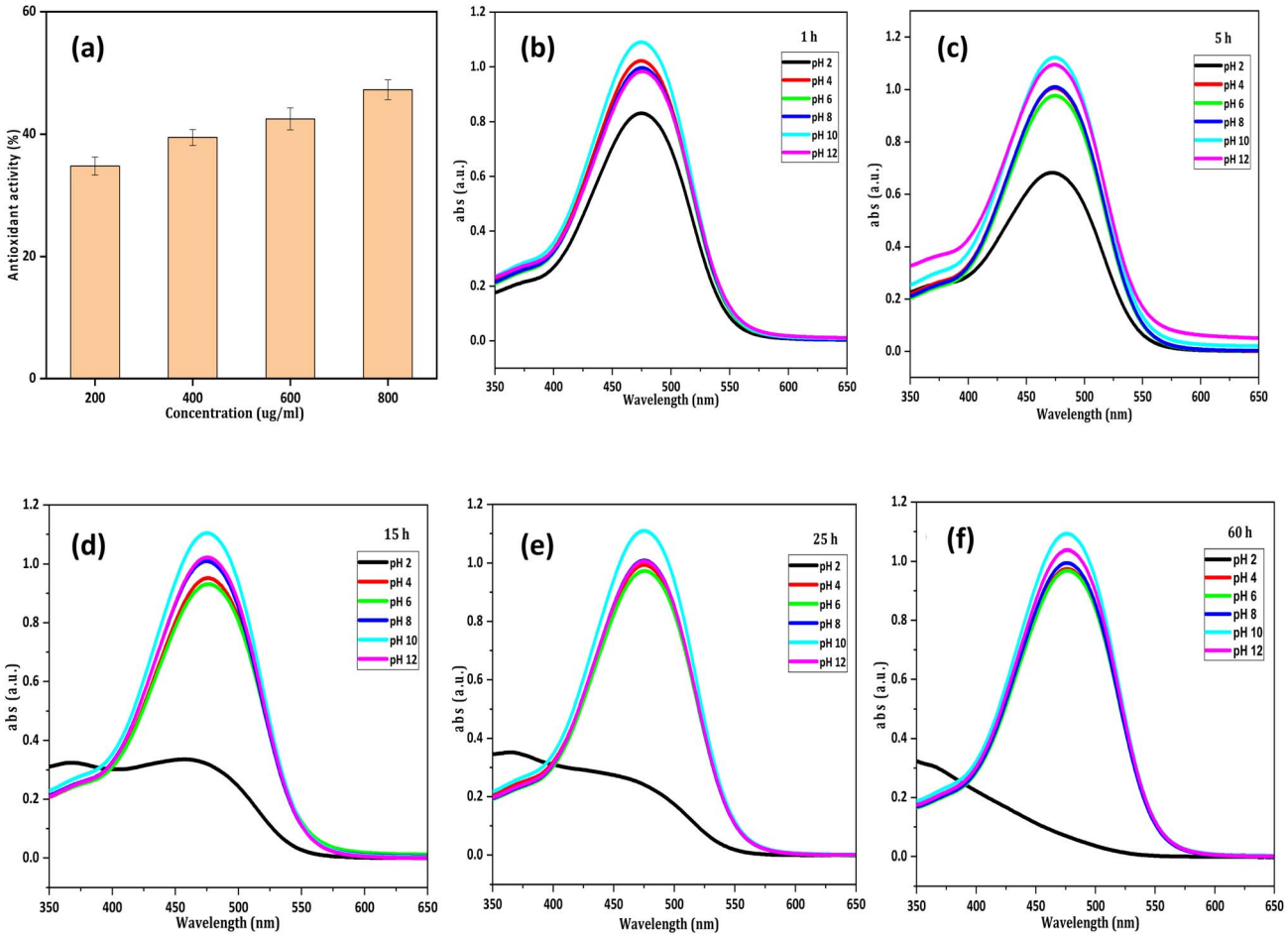

Fig. 7 (a) Antioxidant activity of canthaxanthin and effect of pH on canthaxanthin at (b) 1 h, (c) 5 h, (d) 15 h, (e) 25 h, and (f) 60 h.

bonds. This makes it an excellent antioxidant compound to scavenge DPPH. DPPH is a nitrogen-centered free radical ion. Canthaxanthin transfers an electron from its conjugated π system to scavenge the DPPH[63] resulting in a decrease in the absorbance. Maximum antioxidant (47%) activity was achieved at 800 μg ml^{-1} of canthaxanthin as shown in Fig. 7(a).

3.12 Water activity, HR and CI

The flowability of powder depends upon the amount of water entrapped by that powder.[64] A previous study showed that the flow factor decreased when water activity increased in MD, milk powder and some crystal sugar.[65] Water activity was enhanced when PC was additionally added in CD and MD, which might be due to the enhancement of the free water in these two walled materials. In the case of PVP, no change was observed in the a_w, adding PC in SC led to a decrease in a_w from 0.044 to 0.014, as shown in Table 3; this might be possible due to ionic, hydrophobic interactions between SC and PC which help to reduce the free water.[66] A value of a_w below 0.6 indicated a dehydrated food product, and these food products are less susceptible to chemical and biological degradation as compared to higher a_w food products.[67]

Table 4 Water activity, Hausner ratio and Carr index of canthaxanthin with matrices

Sr. no.	Sample	Water activity(a_w)	Hausner ratio (HR)	Carr index (CI) (%)
1	CD	0.10 ± 0.015	1.75 ± 0.025	43
2	MD	0.05 ± 0.011	1.70 ± 0.02	41
3	SC	0.05 ± 0.015	1.76 ± 0.025	43
4	PVP	0.07 ± 0.005	1.53 ± 0.011	35
5	PC	0.10 ± 0.005	1.75 ± 0.023	42
6	CD–PC	0.15 ± 0.005	1.43 ± 0.005	30
7	MD–PC	0.08 ± 0.011	1.64 ± 0.026	38
8	SC–PC	0.06 ± 0.01	1.69 ± 0.017	41
9	PVP–PC	0.09 ± 0.005	1.60 ± 0.015	38

The CI and HR are the most important parameters of powders. The CI signifies the compressibility, and HR signifies the cohesiveness and packability of powders.[68] A HR value more than 1.25 indicates poor flowability of encapsulated powder. Both the HR (30.55%) and CI (1.44) were minimum for CD–PC encapsulated powder. CD–PC reduces interparticle space thus increasing the bulk volume and reduces both parameters.[68] CD showed good flowability as compared to all other wall materials. PVP and MD showed a CI of 35% and 41.66% respectively, while when these two added with PC, it led to an almost similar value of CI as shown in Table 4.

4 Conclusion

The present study optimized the canthaxanthin production from ATRS. Under optimized conditions, 135 mg l^{-1} of canthaxanthin was produced. NaCl showed enhanced biomass production as compared to other tested salts in fermentation. Ultrasound assisted extraction showed 16.67% more canthaxanthin yield than that without ultrasonication. Purified canthaxanthin showed an antioxidant activity of 47% in DPPH assay and pH stability above pH 2. It was further encapsulated into different host materials. PVP showed the highest EE of 75% and also showed improved release kinetics in the Higuchi model. CD–PC and PVP both showed 30% and 35% Carr index and Hausner ratio respectively. This study not only finds a way for sustainable production of canthaxanthin but also showed the potential application of canthaxanthin in the food and nutraceutical sectors.

Author contributions

Devendra Pratap Singh: writing – original draft, methodology, investigation, data curation, conceptualization; Priyanka: validation, visualization; Tania Raheja: visualization; Saumya Singh: writing – review and editing, conceptualization; Neera Agarwal: writing – review and editing; Meena Krishania: supervision, project administration, writing – review and editing.

Conflicts of interest

The authors have no conflict of interest to declare.

Data availability

Data will be made available on request.

Supplementary information (SI) is available. See DOI: https://doi.org/10.1039/d5fb00696a.

Acknowledgements

The authors are thankful to the BRIC-National Agri-Food and Biomanufacturing Institute (Formerly CIAB) and Department of Biotechnology (DBT), Govt. of India, for their consistent financial support, infrastructure and instrumentation facility.

References

1 I. Castangia, M. L. Manca, S. H. Razavi, A. Nácher, O. Díez-Sales, J. E. Peris, M. Allaw, M. C. Terencio, I. Usach and M. Manconi, Canthaxanthin biofabrication, loading in green phospholipid vesicles and evaluation of in vitro protection of cells and promotion of their monolayer regeneration, *Biomedicines*, 2022, **10**(1), 157, DOI: 10.3390/biomedicines10010157.

2 W. Pyter, J. Grewal, D. Bartosik, L. Drewniak and K. Pranaw, Pigment production by Paracoccus spp. strains through submerged fermentation of valorized lignocellulosic wastes, *Fermentation*, 2022, **8**(9), 440, DOI: 10.3390/fermentation8090440.

3 J. Liu, Y. Luo, T. Guo, C. Tang, X. Chai, W. Zhao, J. Bai and Q. Lin, Cost-effective pigment production by Monascus purpureus using rice straw hydrolysate as substrate in submerged fermentation, *J. Biosci. Bioeng.*, 2020, **129**(2), 229–236, DOI: 10.1016/j.jbiosc.2019.08.007.

4 S. S. Abuthahir, C. K. Venil, M. Malathi and P. R. Devi, Optimization of submerged fermentation for enhanced production of canthaxanthin by Dietzia maris AURCCBT01, *Mater. Today: Proc.*, 2021, **47**, 2132–2137, DOI: 10.1016/j.matpr.2021.05.150.

5 S. Singh, G. Kaur, D. P. Singh, S. K. Arya and M. Krishania, Exploring rice straw's potential from a sustainable biorefinery standpoint: Towards valorization and diverse product production, *Process Saf. Environ. Prot.*, 2024, **184**, 314–331, DOI: 10.1016/j.psep.2024.01.105.

6 R. G. Dingcong Jr, M. A. Ahalajal, L. C. Mendija, R. J. Ruda-Bayor, F. P. Maravillas, A. I. Cavero, E. J. Cea, K. J. Pantaleon, K. J. Tejas, E. A. Limbaga and G. G. Dumancas, Valorization of agricultural rice straw as a sustainable feedstock for rigid polyurethane/polyisocyanurate foam production, *ACS Omega*, 2024, **9**(11), 13100–13111, DOI: 10.1021/acsomega.3c09583.

7 I. G. Mota, R. A. Neves, S. S. Nascimento, B. L. Maciel, A. H. Morais and T. S. Passos, Artificial dyes: Health risks and the need for revision of international regulations, *Food Rev. Int.*, 2023, **39**(3), 1578–1593, DOI: 10.1080/87559129.2021.1934694.

8 M. R. Nasri Nasrabadi and S. H. Razavi, Enhancement of canthaxanthin production from Dietzia natronolimnaea HS-1 in a fed-batch process using trace elements and statistical methods, *Braz. J. Chem. Eng.*, 2010, **27**, 517–529, DOI: 10.1590/S0104-66322010000400003.

9 F. Khodaiyan, S. H. Razavi and S. M. Mousavi, Optimization of canthaxanthin production by Dietzia natronolimnaea HS-1 from cheese whey using statistical experimental methods, *Biochem. Eng. J.*, 2008, **40**(3), 415–422, DOI: 10.1016/j.bej.2008.01.016.

10 S. M. Gharibzahedi, S. H. Razavi and M. Mousavi, Feeding strategies for the improved biosynthesis of canthaxanthin from enzymatic hydrolyzed molasses in the fed-batch fermentation of Dietzia natronolimnaea HS-1, *Bioresour. Technol.*, 2014, **154**, 51–58, DOI: 10.1016/j.biortech.2013.12.013.

11 V. Gaur and S. Bera, Microbial canthaxanthin: an orange-red keto carotenoid with potential pharmaceutical applications, *Biotechnologia*, 2023, **104**(3), 315, DOI: 10.5114/bta.2023.130733 https://www.gminsights.com/industry-analysis/canthaxanthin-market.
12 F. B. Aguilar, B. Dusemund, P. Galtier, J. Gilbert, D. M. Gott, S. Grilli, R. Gürtler, J. König, C. Lambré, J. C. Larsen and J. C. Leblanc, Scientific opinion on the re-evaluation of canthaxanthin (E 161 g) as a food additive, *EFSA J.*, 2010, **8**(10), 1–42, DOI: 10.2903/j.efsa.2010.1852.
13 S. Ghosh, T. Sarkar, A. Das and R. Chakraborty, Natural colorants from plant pigments and their encapsulation: An emerging window for the food industry, *LWT*, 2022, **153**, 112527, DOI: 10.1016/j.lwt.2021.112527.
14 M. T. Arshad, S. Maqsood, A. Ikram, A. A. Khan, A. Raza, A. Ahmad and K. T. Gnedeka, Encapsulation Techniques of Carotenoids and Their Multifunctional Applications in Food and Health: An Overview, *Food Sci. Nutr.*, 2025, **13**(5), e70310, DOI: 10.1002/fsn3.70310.
15 S. Singh, D. Kaur, S. K. Yadav and M. Krishania, Process scale-up of an efficient acid-catalyzed steam pretreatment of rice straw for xylitol production by C. Tropicalis MTCC 6192, *Bioresour. Technol.*, 2021, **320**, 124422, DOI: 10.1016/j.biortech.2020.124422.
16 K. Miglani, S. Singh, D. P. Singh and M. Krishania, Sustainable production of prodigiosin from rice straw derived xylose by using isolated Serratia marcescens (CMS 2): statistical optimization, characterization, encapsulation & cost analysis, *Sustainable Food Technol.*, 2023, **1**(6), 837–849, DOI: 10.1039/D3FB00100H.
17 S. Sun, W. Chen, J. Tang, B. Wang, X. Cao, S. Sun and R. C. Sun, Synergetic effect of dilute acid and alkali treatments on fractional application of rice straw, *Biotechnol. Biofuels*, 2016, **9**(1), 217, DOI: 10.1186/s13068-016-0632-9.
18 M. S. Abdel-Salam, S. S. Hafez, M. Fadel, S. A. Mohamed, W. K. Hegazy and B. E. Khalil, Bio ethanol production from rice straw saccharification via avicelase gene in E. coli recombinant strain, *Clean Technol.*, 2023, **5**(2), 451–465, DOI: 10.3390/cleantechnol5020023.
19 W. Nachaiwieng, A. Kanpiengjai, T. Watanabe and C. Khanongnuch, *Influences of buffer systems on enzymatic saccharification of rice husk holocellulose and fermenting ability of various ethanol producing microorganisms*, Chiang Mai University, Thailand, 2015.
20 B. Padhan, K. Poddar, D. Sarkar and A. Sarkar, Production, purification, and process optimization of intracellular pigment from novel psychrotolerant Paenibacillus sp. BPW19, *Biotechnol. Rep.*, 2021, **29**, e00592, DOI: 10.1016/j.btre.2021.e00592.
21 M. Krępska, K. Sieczyńska and M. Lasoń-Rydel, Determination of astaxanthin and canthaxanthin in food products by HPLC method, *Technologia i Jakość Wyrobów*, 2022, **67**, 106–116.
22 J. Cvejic, S. Tambutté, S. Lotto, M. Mikov, I. Slacanin and D. Allemand, Determination of canthaxanthin in the red coral (Corallium rubrum) from Marseille by HPLC combined with UV and MS detection, *Mar. Biol.*, 2007, **152**(4), 855–862, DOI: 10.1007/s00227-007-0738-5.
23 L. Mahalakshmi, M. M. Leena, J. A. Moses and C. Anandharamakrishnan, Micro-and nano-encapsulation of β-carotene in zein protein: Size-dependent release and absorption behavior, *Food Funct.*, 2020, **11**(2), 1647–6, DOI: 10.1039/C9FO02088H.
24 A. Saifi, J. P. Joseph, A. P. Singh, A. Pal and K. Kumar, Complexation of an azo dye by cyclodextrins: a potential strategy for water purification, *ACS Omega*, 2021, **6**(7), 4776–4782, DOI: 10.1021/acsomega.0c05684.
25 R. Liu, X. Wang, L. Yang, Y. Wang and X. Gao, Coordinated encapsulation by β-cyclodextrin and chitosan derivatives improves the stability of anthocyanins, *Int. J. Biol. Macromol.*, 2023, **242**, 125060, DOI: 10.1016/j.ijbiomac.2023.125060.
26 K. Li, H. Zhao, X. He, C. Sun, R. Xu and Q. Li, Ca^{2+}-mediated chitosan/sodium alginate encapsulated Red Monascus Pigment hydrogel beads: Preparation, characterization and release kinetics, *Int. J. Biol. Macromol.*, 2024, **277**, 134380, DOI: 10.1016/j.ijbiomac.2024.134380.
27 N. Seyedrazi, S. H. Razavi and Z. Emam-Djomeh, Effect of different pH on canthaxanthin degradation, *Eng. Technol.*, 2011, **59**, 532–536.
28 N. Ćujić Nikolić, M. Jovanović, M. Radan, Z. Lazarević, D. Bigović, S. Marković, N. Jovanović Lješković and K. Šavikin, Development of cyclodextrin-based mono and dual encapsulated powders by spray drying for successful preservation of everlasting flower extract, *Pharmaceutics*, 2024, **16**(7), 861, DOI: 10.3390/pharmaceutics16070861.
29 P. Sruthi, M. M. Naidu and P. J. Rao, Valorization of cashew nut testa phenolics through nano-complexes stabilized with whey protein isolate and β-cyclodextrin: Characterization, anti-oxidant activity, stability and in vitro release, *Food Res. Int.*, 2024, **181**, 114110, DOI: 10.1016/j.foodres.2024.114110.
30 S. M. Gharibzahedi, S. H. Razavi, S. M. Mousavi and V. Moayedi, High efficiency canthaxanthin production by a novel mutant isolated from Dietzia natronolimnaea HS-1 using central composite design analysis, *Ind. Crops Prod.*, 2012, **40**, 345–354, DOI: 10.1016/j.indcrop.2012.03.030.
31 K. Weerasai, N. Suriyachai, A. Poonsrisawat, J. Arnthong, P. Unrean, N. Laosiripojana and V. Champreda, Sequential Acid and Alkaline Pretreatment of Rice Straw for Bioethanol Fermentation, *BioResources*, 2014, **9**(4), 5988–6001, DOI: 10.15376/biores.9.4.5988-6001.
32 W. L. Sun and W. Y. Tao, Simultaneous saccharification and fermentation of rice straw pretreated by a sequence of dilute acid and dilute alkali at high dry matter content, *Energy Sources, Part A*, 2013, **35**(8), 741–752, DOI: 10.1080/15567036.2010.514649.
33 P. Zhang, Z. Li, L. Lu, Y. Xiao, J. Liu, J. Guo and F. Fang, Effects of stepwise nitrogen depletion on carotenoid content, fluorescence parameters and the cellular stoichiometry of Chlorella vulgaris, *Spectrochim. Acta, Part A*, 2017, **181**, 30–38, DOI: 10.1016/j.saa.2017.03.022.
34 A. Gandhi, Y. Cui, M. Zhou and N. P. Shah, Effect of KCl substitution on bacterial viability of Escherichia coli (ATCC

25922) and selected probiotics, *J. Dairy Sci.*, 2014, **97**(10), 5939–5951, DOI: 10.3168/jds.2013-7681.

35 G. Mattar, A. Haddarah, J. Haddad, M. Pujola and F. Sepulcre, Are citric acid-iron II complexes true chelates or just physical mixtures and how to prove this?, *Foods*, 2023, **12**(2), 410, DOI: 10.3390/foods12020410.

36 E. Palmqvist and B. Hahn-Hägerdal, Fermentation of lignocellulosic hydrolysates. II: inhibitors and mechanisms of inhibition, *Bioresour. Technol.*, 2000, **74**(1), 25–33, DOI: 10.1016/S0960-8524(99)00161-3.

37 G. Goswami, S. Chakraborty, S. Chaudhuri and D. Dutta, Optimization of process parameters by response surface methodology and kinetic modeling for batch production of canthaxanthin by Dietzia maris NIT-D (accession number: HM151403), *Bioproc. Biosyst. Eng.*, 2012, **35**(8), 1375–1388, DOI: 10.1007/s00449-012-0726-0.

38 F. Rostami, S. H. Razavi, A. A. Sepahi and S. M. Gharibzahedi, Canthaxanthin biosynthesis by Dietzia natronolimnaea HS-1: effects of inoculation and aeration rate, *Braz. J. Microbiol.*, 2014, **45**, 447–456, DOI: 10.1590/s1517-83822014005000046.

39 A. G. Demesa, S. Saavala, M. Pöysä and T. Koiranen, Overview and toxicity assessment of ultrasound-assisted extraction of natural ingredients from plants, *Foods*, 2024, **13**(19), 3066, DOI: 10.3390/foods13193066.

40 M. Hojjati, S. H. Razavi, K. Rezaei and K. Gilani, Stabilization of canthaxanthin produced by Dietzia natronolimnaea HS-1 with spray drying microencapsulation, *J. Food Sci. Technol.*, 2014, **51**(9), 2134–2140, DOI: 10.1007/s13197-012-0713-0.

41 T. Esatbeyoglu and G. Rimbach, Canthaxanthin: From molecule to function, *Mol. Nutr. Food Res.*, 2017, **61**(6), 1600469, DOI: 10.1002/mnfr.201600469.

42 V. Venugopalan, S. K. Tripathi, P. Nahar, P. P. Saradhi, R. H. Das and H. K. Gautam, Characterization of canthaxanthin isomers isolated from a new soil Dietzia sp. and their antioxidant activities, *J. Microbiol. Biotechnol.*, 2013, **23**(2), 237–245, DOI: 10.4014/jmb.1203.03032.

43 T. Maoka, Carotenoids: distribution, function in nature, and analysis using LC-photodiode array detector (DAD)-MS and MS/MS system, *Mass Spectrom.*, 2023, **12**(1), A0133, DOI: 10.5702/massspectrometry.A0133.

44 B. Emadzadeh, B. Ghorani, S. Naji-Tabasi, E. Charpashlo and M. Molaveisi, Fate of β-cyclodextrin-sugar beet pectin microcapsules containing garlic essential oil in an acidic food beverage, *Food Biosci.*, 2021, **42**, 101029, DOI: 10.1016/j.fbio.2021.101029.

45 A. Karimloo, S. H. Razavi and S. M. Mousavi, Improving the antioxidant activity of microbial canthaxanthin by its encapsulation with bioactive peptides of soybean protein, *Food Biosci.*, 2023, **56**, 103319, DOI: 10.1016/j.fbio.2023.103319.

46 M. Arab, S. M. Hosseini, K. Nayebzadeh, N. Khorshidian, M. Yousefi, S. H. Razavi and A. M. Mortazavian, Microencapsulation of microbial canthaxanthin with alginate and high methoxyl pectin and evaluation the release properties in neutral and acidic condition, *Int. J. Biol. Macromol.*, 2019, **121**, 691–698, DOI: 10.1016/j.ijbiomac.2018.10.114.

47 A. Kozioł, K. Środa-Pomianek, A. Górniak, A. Wikiera, K. Cyprych and M. Malik, Structural determination of pectins by spectroscopy methods, *Coatings*, 2022, **12**(4), 546, DOI: 10.3390/coatings12040546.

48 L. Chen, S. Yang, Z. Nan, Y. Li, J. Ma, J. Ding, Y. Lv and J. Yang, Detection of dextran, maltodextrin and soluble starch in the adulterated Lycium barbarum polysaccharides (LBPs) using Fourier-transform infrared spectroscopy (FTIR) and machine learning models, *Heliyon*, 2023, **9**(6), e17115, DOI: 10.1016/j.heliyon.2023.e17115.

49 A. Synytsya, J. Copiková, P. Matějka and V. J. Machovič, Fourier transform Raman and infrared spectroscopy of pectins, *Carbohydr. Polym.*, 2003, **54**(1), 97–106, DOI: 10.1016/S0144-8617(03)00158-9.

50 A. Rahma, M. M. Munir, A. Prasetyo, V. Suendo and H. Rachmawati, Intermolecular interactions and the release pattern of electrospun curcumin-polyvinyl (pyrrolidone) fiber, *Biol. Pharm. Bull.*, 2016, **39**(2), 163–173, DOI: 10.1248/bpb.b15-00391.

51 M. Hojjati, S. H. Razavi, K. Rezaei and K. Gilani, Spray drying microencapsulation of natural canthaxantin using soluble soybean polysaccharide as a carrier, *Food Sci. Biotechnol.*, 2011, **20**(1), 63–69, DOI: 10.1007/s10068-011-0009-6.

52 Q. Hu, L. Huang, J. Wang, J. Huangfu, Y. Cai, T. Liu, M. Zhao and Q. Zhao, Characterization of sodium caseinate derived from various sources: unraveling the relationship between structure and functional properties, *Food Biosci.*, 2024, **61**, 104570, DOI: 10.1016/j.fbio.2024.104570.

53 R. P. Reksamunandar, D. Edikresnha, M. M. Munir and S. Damayanti, Encapsulation of β-carotene in poly (vinylpyrrolidone)(PVP) by electrospinning Technique, *Procedia Eng.*, 2017, **170**, 19–23, DOI: 10.1016/j.proeng.2017.03.004.

54 X. Han, Z. Zhang, H. Shen, J. Zheng and G. Zhang, Comparison of structures, physicochemical properties and in vitro bioactivity between ferulic acid-β-cyclodextrin conjugate and the corresponding inclusion complex, *Food Res. Int.*, 2019, **125**, 108619, DOI: 10.1016/j.foodres.2019.108619.

55 K. A. Silva, M. A. Coelho, V. M. Calado and M. H. Rocha-Leão, Olive oil and lemon salad dressing microencapsulated by freeze-drying, *LWT-Food Sci. Technol.*, 2013, **50**(2), 569–574, DOI: 10.1016/j.lwt.2012.08.005.

56 Y. R. Kang, Y. K. Lee, Y. J. Kim and Y. H. Chang, Characterization and storage stability of chlorophylls microencapsulated in different combination of gum Arabic and maltodextrin, *Food Chem.*, 2019, **272**, 337–346, DOI: 10.1016/j.foodchem.2018.08.063.

57 H. Zhang, C. Jia, Y. Xiao, J. Zhang, J. Yu, X. Li, N. Hamid and A. Sun, Enhanced stability and bioavailability of mulberry anthocyanins through the development of sodium caseinate-konjac glucomannan nanoparticles, *Food Chem.*, 2024, **439**, 138150, DOI: 10.1016/j.foodchem.2023.138150.

58 M. H. Mahmoud, F. M. Abu-Salem and D. E. Azab, A comparative study of pectin green extraction methods from apple waste: characterization and functional properties, *Int. J. Food Sci.*, 2022, **2022**(1), 2865921, DOI: 10.1155/2022/2865921.

59 J. Rao, C. Shen, Z. Yang, O. A. Fawole, J. Li, D. Wu and K. Chen, Facile microfluidic fabrication and characterization of ethyl cellulose/PVP films with neatly arranged fibers, *Carbohydr. Polym.*, 2022, **292**, 119702, DOI: 10.1016/j.carbpol.2022.119702.

60 P. Sharayei, E. Azarpazhooh, S. Einafshar, S. Zomorodi, F. Zare and H. S. Ramaswamy, Optimization of wall materials for astaxanthin powder production from shrimp shell extract using simplex lattice mixture design, *J. Food Process. Preserv.*, 2024, **2024**(1), 9794290, DOI: 10.1155/2024/9794290.

61 F. Navab, A. Rezaei, M. H. Rouhani, F. Shahdadian and M. Alikord, Vitamin D3 capsulation using maillard reaction complex of sodium caseinate and tragacanth gum, *Food Chem.: X*, 2024, **24**, 101910, DOI: 10.1016/j.fochx.2024.101910.

62 A. Mortensen and L. H. Skibsted, Kinetics and mechanism of the primary steps of degradation of carotenoids by acid in homogeneous solution, *J. Agric. Food Chem.*, 2000, **48**(2), 279–286, DOI: 10.1021/jf9904620.

63 L. Yang, X. Qiao, J. Liu, L. Wu, Y. Cao, J. Xu and C. Xue, Preparation, characterization and antioxidant activity of astaxanthin esters with different molecular structures, *J. Sci. Food Agric.*, 2021, **101**(6), 2576–2583, DOI: 10.1002/jsfa.10887.

64 E. Juarez-Enriquez, G. I. Olivas, E. Ortega-Rivas, P. B. Zamudio-Flores, S. Perez-Vega and D. R. Sepulveda, Water activity, not moisture content, explains the influence of water on powder flowability, *LWT*, 2019, **100**, 35–39, DOI: 10.1016/j.lwt.2018.10.043.

65 E. Ostrowska-Ligęza and A. Lenart, Influence of water activity on the compressibility and mechanical properties of cocoa products, *LWT-Food Sci. Technol.*, 2015, **60**(2), 1054–1060, DOI: 10.1016/j.lwt.2014.10.040.

66 C. Murru, M. A. Mohammadifar, J. B. Wagner, R. Badía Laiño and M. E. Díaz García, High methoxyl pectin and sodium caseinate film matrix reinforced with green carbon quantum dots: rheological and mechanical studies, *Membranes*, 2022, **12**(7), 695, DOI: 10.3390/membranes12070695.

67 E. Sandulachi, Water activity concept and its role in food preservation, *J. Eng. Sci.*, 2012, **1**(4), 40–48.

68 M. Radan, N. Ćujić Nikolić, S. Kuzmanović Nedeljković, Z. Mutavski, N. Krgović, T. Stević, S. Marković, A. Jovanović, J. Živković and K. Šavikin, Multifunctional pomegranate peel microparticles with health-promoting effects for the sustainable development of novel nutraceuticals and pharmaceuticals, *Plants*, 2024, **13**(2), 281, DOI: 10.3390/plants13020281.